Available online at www.sciencerepository.org

Science Repository

Research Article

Electrospun Nanofibrous Poly(3-Hydroxybutyrate-Co-3-Hydroxyvalerate) With Antibacterial Activity

Etienne Dessauw[1], Samir Abbad Andaloussi[2], Davy Louis Versace[1], Estelle Renard[1] and Valérie Langlois[1*]

[1]Institut de Chimie et des Matériaux de Paris-Est, UMR 7182, CNRS-UPEC, 2-8 rue Henri Dunant, 94320 Thiais, France
[2]Laboratoire Eau Environnement et Systèmes Urbains (LEESU), Université Paris-Est, 61 avenue du Général de Gaulle, 94010 Créteil cedex, France

ARTICLEINFO

Article history:
Received: 19 June, 2019
Accepted: 9 August, 2019
Published: 17 August, 2019

Keywords:
poly (hydroxyalkanoate)
PHBHV
electrospinning
antibacterial activity
antiradical property

ABSTRACT

Elaboration of electrospun nanofibrous poly(3-hydroxybutyrate-co-3-hydroxyvalerate) (PHBHV)-based mats was implemented through two routes to obtain antibacterial material containing carvacrol, a phenolic compound extracted from essential oils. The first strategy relied on a direct blend of PHBHV and carvacrol/β-cyclodextrin inclusion complexes, PHBHV (carvCD-IC), while the second approach implied the elaboration of multilayered scaffold *via* the introduction of poly(β-CD-epichlorohydrin), PolyCD. The PolyCD/carv-based mat was electrospun between two hydrophobic PHBHV mats. Scanning Electron Microscopy analysis of mats showed uniform and beadless fibers. The three layered materials [PHBHV-(PolyCD/carv)-PHBHV] is sufficient to ensure optimal antiradical activity (RSA of 88.6%) and exhibit interesting antibacterial activities against *E. coli* and *S. aureus*.

Introduction

Poly(3-hydroxyalkanoates) (PHAs) are a class of natural biodegradable polyesters accumulated by many bacteria as carbon and energy supply when an essential nutrient is limited. Using various substrates, a wide variety of PHAs are synthesized, differing notably by the length of the side chains [1-3]. Among them, the poly(3-hydroxybutyrate-co-3-hydroxyvalerate) PHBHV having lateral short chain lengths is the most widely known. Thanks to their biocompatibility and biodegradability, PHAs proved to be good candidates for medical applications including biomedical devices, degradable drug carriers or for tissue engineering [4-16]. Electrospinning is a suitable technique to obtain PHA nanofibers (NFs) that have been used as biocompatible scaffold [17-20]. To improve the properties of electrospun NFs, chemical modifications have been carried out, bioactive molecules are directly incorporated into the fibers or deposited at the surface of the NFs by the combined electropinning/electrospraying process [18, 19, 21, 22]. Due to the emergence of antibiotic-resistant bacteria, the development of new antibacterial agents has become more than necessary. The exploration of natural resources appears to be one of the most promising because they constitute a large reserve of bioactive substances [23, 24]. The active molecules, involved in the defensive mechanisms of plants are mostly concentrated in essential oils. The exploration of essential oils for the search for molecules with antibacterial activity therefore seems to be an interesting approach. The constituents of essential oils can be divided into two classes according to their biosynthetic pathway, the terpenoids and the phenylpropanoids. Among them carvacrol (5-isopropyl-2-methylphenol) extracted from oregano exhibits antibacterial, antifungal, antiviral, antitumor and anti-inflammatory properties [25-28]. Entrapment of carvacrol by polymeric particles or molecular encapsulation by hydrophobic cavity of β-cyclodextrin (CD) have been used to extend its stability against evaporation and degradation [29-34]. The CD, produced from starch by an enzymatic process is a cyclic oligosaccharide able to form non-covalent host guest inclusion complex (CD-IC) with a variety of nonpolar molecules such as antioxidant, fragrance and essential oils [35]. Carvacrol is really included inside the lipophilic CD cavity. The intermolecular hydrogen interactions in the carvacrol/CD-IC play an essential role with regard to the stability of these complexes. Concerning the orientation inside the CD cavity it has been shown that the methyl group of carvacrol is oriented toward the narrower rim of the CD cavity whereas the isopropyl group points to the

Correspondence to: Valérie Langlois, Institut de Chimie et des Matériaux de Paris-Est, UMR 7182, CNRS-UPEC, 2-8 rue Henri Dunant, 94320 Thiais, France; Tel: 33 (0)1 49 78 12 17. E-mail: langlois@icmpe.cnrs.fr

http://dx.doi.org/10.31487/j.JBEM.2019.01.02

wider rim [34, 36, 37]. Carvacrol/modified-cyclodextrin inclusion complex fibers (carvacrol/CD-IC fibers) were recently produced *via* electrospinning and nanofibres have shown fast-dissolving properties in water [38].

In this context, the unique properties of biocompatible PHA nanofibers and the performance of the carvacrol/β-cyclodextrin inclusion complexes (carv/CD-IC) systems are promising strategies to both combine antibacterial activity and biocompatibility of materials. The carv/CD-IC (Figure 1) were prepared and characterized by ^{1}H NMR, XRD and TGA analysis. Nanofibers based on PHBHV and carv/CD-IC were prepared by electrospinning in one step. In the objective to enhance content of carvacrol, β-cyclodextrin polymer, PolyCD, prepared by reaction between CD and epichlorohydrin under basic conditions, has been used. Due to its solubility in water, multilayered materials were prepared by combining two layers of hydrophobic PHBHV containing a layer of PolyCD inside in a three steps electrospinning processes (Figure 2) [39]. Materials were analyzed by SEM, TGA and XRD. The influence of the proportion of the carv/CD-IC on thermal and morphological structure of the nanofibers was reported and their actions against the adhesion of both pathogenic bacteria strains *Staphylococcus aureus* and *Escherichia coli* were evaluated.

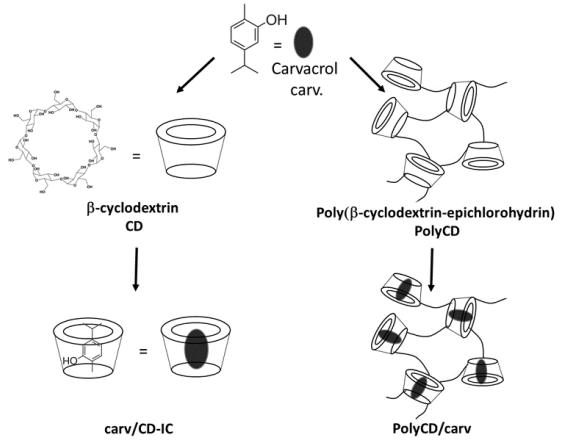

Figure 1: Chemical structures of carvacrol/CD-Inclusion complex and polyCD/carvacrol

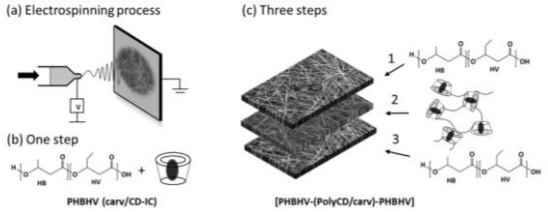

Figure 2: Schematic representations (a) electrospinning process (b) formation of PHBHV(carv/CD-IC) in one step (c) formation of 3-layered electrospun [PHBHV-(PolyCD/carv)-PHBHV]

Experimental part

I Materials

Poly(3-hydroxybutyrate-co-3-hydroxyvalerate) (PHBHV) containing 12 mol % hydroxyvalerate (HV) with average Mw =210 000 g.mol^{-1} was purchased from Goodfellow. β-CD was purchased from Roquette. Carvacrol, chloroform, N, N-dimethylformamide anhydrous, methanol, 2,2-diphenyl-1-picrylhydrazyl (DPPH), Lysogeny Broth, Miller (LB medium) and all solvents were purchased from Sigma-Aldrich and used without purification. The high molar mass CD-epichlorohydrin polymer, PolyCD, was prepared by reaction between CD and epichlorohydrin under basic conditions [41].

II Preparation of inclusion complex, carv/CD-IC

The inclusion complexes of carv/CD-IC were prepared using co-precipitation method in 1:1 molar ratio. CD solution was prepared by dissolving 3.64 g of CD in 200 mL of water (18.2 g.L^{-1}) and then 481.9 mg of carvacrol was added slowly and a suspension was formed. The suspension was kept under stirring at 30°C during 48 hours. Suspension of inclusion complexes was freeze-dried or filtered under 2 bars of pressure with stainless steel pressure filter holder through a 0.2 µm membrane filter. Inclusion complexes were then dried under vacuum at 60°C during 16 hours.

III Entrapment efficiency (EE)

The entrapment efficiency was determined by UV-vis spectroscopy at 274 nm, Varian Cary 50 Bio UV–Visible spectrophotometer. Calibration curve was plotted using carvacrol concentration ranging from 0.028 to 0.064 g.L^{-1}. To determine total amount of carvacrol from inclusion complexes, 5 mg of inclusion complexes were dissolved in 5 mL of acetonitrile during 48h at room temperature to allow all entrapped carvacrol to be in solution, providing the total carvacrol from inclusion complexes (entrapped and surface-adsorbed). To determine the amount of carvacrol adsorbed at the surface of inclusion complexes, 0.5 g of inclusion complexes was washed in 5 mL of acetonitrile for 20 min. Solutions were then centrifuged at 3200 x g for 15 min to separate carvacrol adsorbed from inclusion complexes. The EE was calculated according to Equation 1:

Equation (1):

$$EE = \frac{(Total\ amount\ of\ carvacrol - surface\ adsorbed\ carvacrol)}{Initial\ amount\ of\ carvacrol} \times 100$$

IV Electrospinning

$PHBHV_{91}(carv/CD\text{-}IC)_9$ scaffolds were obtained by electrospinning a mixture of 23% (w/v) PHBHV solution with 9 wt.% of carv/CD-IC. The concentration of the solution was 253 g.L^{-1}. [PHBHV-(PolyCD/carv)-PHBHV] multilayered materials were prepared as follows: the first layer was obtained by electrospinning a 23 % (w/v) PHBHV solution, the second layer was obtained by electrospinning the solution of polyCD (89 wt.%) complexed with carvacrol (11 wt.%) in DMF (897 g.L^{-1}), and then another electrospun PHBHV layer. For all the mixtures, PHBHV was dissolved overnight in a 85/15 (v/v) ratio of $CHCl_3$/DMF before adding

the CD or carv/CD-IC. The electrospun fibers were obtained using a Fluidnatek® LE-10 electrospinning apparatus manufactured by Bioinicia S.L., Valencia, Spain. The suspensions were processed by a single phase nozzle with scanning motion through one concentric stainless-steel needles (0.9 mm of outer diameters). The tool was operated under a steady flow-rate using a motorized syringe pump system and equipped with a variable high-voltage 0-31 kV power supply. Briefly, the polymer mixtures were placed in a 20 mL syringe and nanofibers were collected onto a stainless-steel plate collector recovered of foil connected to the ground electrode of the power supply and placed at a tip-to-collector distance of 15 or 25 cm at a variable flow rate of 1-1.5 mL h^{-1}; a voltage of 25-31 kV was applied. The experiments were carried out at room temperature.

V Test DPPH

The radical scavenging activity (RSA) of the networks was determined by using DPPH (2,2-diphenyl-1-picrylhydrazyl) [40]. 50 mg of the samples were immersed in 4 mL of 0.1 mM of DPPH solution in methanol in the dark for 60 min at room temperature. The RSA was measured by using a Varian Cary 50 Bio UV–Visible spectrophotometer controlled by the CaryWinUV software. The DPPH solution is well known to have a maximum of absorption at 517 nm. RSA was therefore determined by monitoring the decrease of the absorbance at this wavelength. RSA was calculated according to the following Equation 2.

Equation (2) $$\text{RSA}\ (\%) = \left(\frac{A_{ref} - A_s}{A_{ref}}\right) \times 100$$

where A_{ref} corresponds to the absorbance of the 0.1 mM of DPPH solution without sample and A_s corresponds to the absorbance of the 0.1 mM solution of DPPH with 50 mg samples of electrospun scaffolds at 517 nm.

VI Microbial Growth Inhibition

The samples of electrospun scaffolds (1 cm^2) were immersed 6 h at 37 °C and stirred (130 rpm) in the bacterial suspension containing *E. coli* or *S. aureus*. 100 µL are taken to measure the absorbance at 600 nm every hour for 6h and at 24h. Experiments were conducted in three replicates. The ANalysis Of the VAriance (ANOVA) statistical test was used and significant differences ($p < 0.05$) among antibacterial properties of the scaffolds were detected thanks to the least significant difference method (LSD) of Fisher.

VII Characterization

The thermal and decomposition characteristics of the materials were determined by thermal gravimetric analyses (TGA) on a Setaram Setsys Evolution 16 apparatus, with a temperature range of 20-800 °C and a heating rate of 10 °C/min. ^{1}H-NMR spectra were recorded on a Bruker Avance II NMR spectrometer 400 MHz. The morphology of the nanofibers was investigated using a Merlin Zeiss scanning electron microscopy. Images were recorded with an acceleration voltage of 5 keV. Prior to analyses, the samples were sputter-coated with a 3nm layer of Pt/Pd in a Cressington 208 HR sputter-coater. The thickness of the metallic layer was monitored by a MTM-20 Cressington quartz balance. The average fiber diameter and porosity were calculated from SEM images using ImageJ software coupled with DiameterJ plugin, a validated nanofiber diameter characterization tool, developed at the National Institute of Standards and Technology. For rheological studies, TA Instruments Advanced Rheometer AR1000 was used with a cone-and-plate geometry of 40 mm diameter and 0.01 rad angle. The geometry was equipped with a solvent trap filled with water and a solvent trap cover in order to limit evaporation and thus concentration changes during long time experiments. All measurements were carried out at room temperature.

Results and discussion

I Preparation and characterization of the carv/CD-Inclusion Complexes, carv/CD-IC and polyCD/carv

The carv/CD-IC prepared by direct co-precipitation were then collected by pressure filtration or by freeze-drying method. Although the filtration method gives a lower yield (65% against 99%) due to the solubility of free CD in water, this process is the more adapted method to obtain inclusion complexes because the entrapment efficiency is higher (95%) than those obtained by freeze-drying method (71%). The chemical shifts (Δδ) of the aromatic protons between the free carvacrol and the complexed carvacrol determined by ^{1}H NMR were calculated as it was previously reported in order to observe the interactions between the complexed compounds and the cavity of the CD (Table 1) [31]. The slight shifts of CD protons noted 3 and 5 of 0.08 and 0.16 ppm respectively combined to the shifts observed for carvacrol protons a, d and e of 0.14, 0.15 and 0.13 ppm (Figure 3) showed significant interactions between the CD and the carvacrol that are characteristic host guest inclusion complex formation. The carv/CD-IC stoichiometry was determined by the ratio of the integration of the peak at 2.2 ppm corresponding to methyl group f of carvacrol and 5.0 ppm corresponding to proton 1 of the CD. Stoichiometries were (1:0.93) and (1:0.94) for the complexes obtained by pressure filtration and freeze-drying methods respectively. In presence of carvacrol, the ^{1}H NMR spectrum also provides evidence for the formation of an inclusion complex with the polyCD (Figure 4) (Table 1). The chemical shifts (Δδ) of the aromatic protons between the free carvacrol and the complexed carvacrol attest significant interactions between polyCD and carvacrol. Furthermore, these signals enlarged in complexed state which was consistent with that above reported for native CD. At the same time, the shape of the signal present in the range 3.3 to 4.5 ppm corresponding to 6 protons of CD and those of 5 protons of epichlorohydrin residues confirmed the inclusion complex. Diffractograms of native CD and carv/CD-IC (Figure 5) showed diffraction peaks in the range of 2θ = 10-35°. The characteristic peaks observed for XRD pattern of CD at 12.6 and 18.3° correspond to the cage-type packing according to previous studies [41, 42]. The XRD pattern carv/CD-IC showed that the crystalline structure of CD has been modified due to the interactions between carvacrol and CD. The intense peaks at 12° and 17.5° and 18.1° respectively are characteristic of channel-type packing which confirms the inclusion complexation of carvacrol inside the CD. Thermal stability of carv/CD-IC was studied by TGA (Figure 6). The major mass loss at around 320°C corresponded to the degradation of the CD. The evaporation of carvacrol shifted from 168°C to 270°C (about 13.6% mass loss) when it is inside the CD as it was previously reported in the case of other host guest interactions in the

CD-IC complex [43-45]. The loss mass of 13.6% of carvacrol observed is similar to the amount of carvacrol introduced during the preparation of inclusion complexes. These results are in agreement with XRD and NMR results.

Table 1: Chemical shifts (δ) of CD, carv/CD-IC and polyCD/carv in D_2O solution using NMR ^1H

Protons	**Free state δ (ppm)**	**Complexed state δ (ppm)**	**$\Delta\delta_{\text{free-complexed}}$ (ppm)**	**Chemical structure**
CD				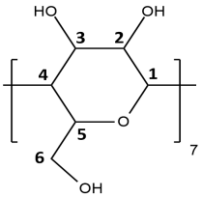
1	5.06	5.03	0.03	
2	3.64	3.62	0.02	
3	3.96	3.88	0.08	
4	3.58	3.57	0.01	
5	3.85	3.69	0.16	
6	3.87	3.78	0.09	
carvacrol		carv/CD-IC		
a	6.80	6.66	0.14	
b	2.82	2.80	0.02	
c	1.17	1.24	-0.07	
d	6.83	6.68	0.15	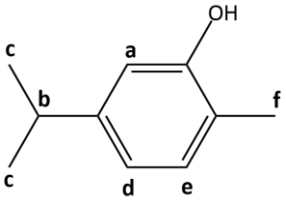
e	7.13	7.00	0.13	
f	2.15	2.17	-0.02	
carvacrol		polyCD/carv		
a	6.80	6.68	0.12	
b	2.82	2.80	0.02	
c	1.17	1.26	-0.09	
d	6.83	6.68	0.15	
e	7.13	7.04	0.09	
f	2.15	2.20	-0.05	

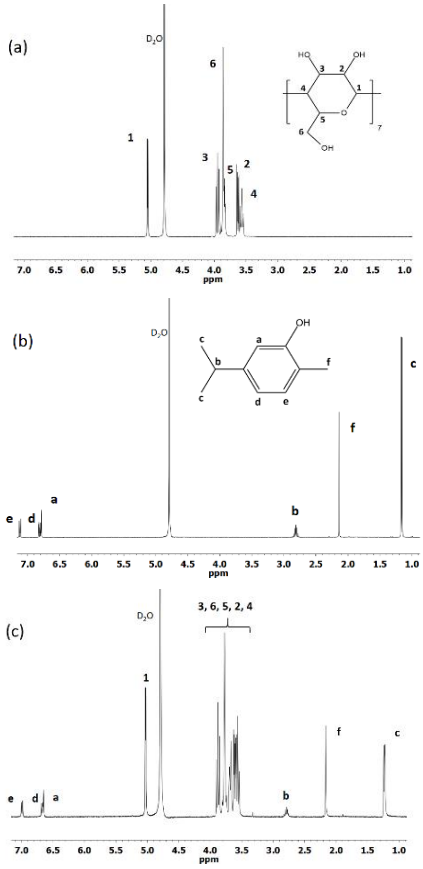

Figure 3: ^1H NMR spectra (a) CD, (b) carvacrol, (c) carv/CD-IC

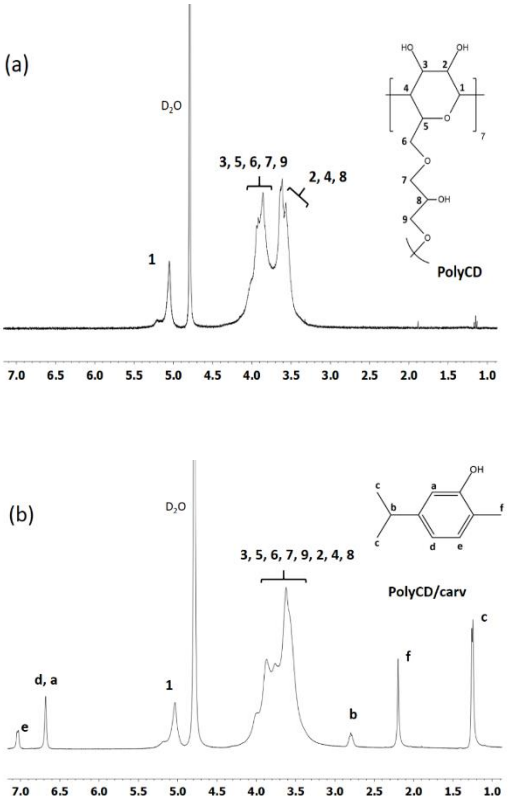

Figure 4: ^1H NMR spectra of (a) polyCD, (b) polyCD/carv

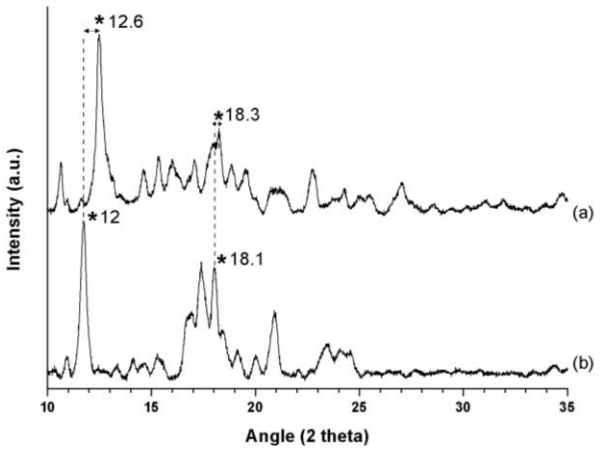

Figure 5: XRD patterns of CD (a) and carv/CD-IC (b)

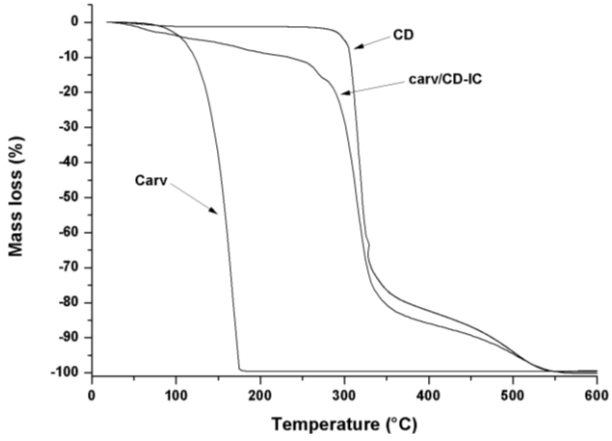

Figure 6: TGA curves of native CD, carv and carv/CD-IC

II Elaboration of electrospun materials

The use of the mixture of two solvents for the electrospinning process is necessary due to the difference of the PHBHV and carv/CD-IC polarities. PHBHV is a very hydrophobic polyester mainly soluble in $CHCl_3$ whereas carv/CD-IC is soluble in DMF. As a consequence, PHBHV was solubilized in a $CHCl_3$/DMF 85/15 (v/v) mixture and it was also previously shown that DMF increased the conductivity of the solution thus promoting the formation of homogeneous and beadless PHBHV fibers by electrospinning [18-20]. The polymer concentration needs to be precisely determined because the morphology of the fibers is closely related to the viscosity of the polymer solution [20, 46]. At 150 $g.L^{-1}$, the viscosity (135 cP) is not enough and the resulting mat shows defects in the form of beads. As the concentration of the PHBHV increases the diameter increases (Table 2). At 230 $g.L^{-1}$, the fibers are homogeneous with very few defects and high fiber diameter (465 ± 172 nm). The viscosity (2550 cP) is sufficient to obtain homogeneous fibers with very few defects. For the blend $PHBHV_{91}CD_9$, homogeneous and flawless fibers were obtained at a concentration of 253 $g.L^{-1}$. Above 9 wt% of CD, the syringe was blocked by the suspension and electrospinning was impossible due to precipitation of CD. Nevertheless, the introduction of carv/CD-IC improves the electrospinning process and it is then possible to introduce up to 17 wt% of carv/CD-IC. The optimal morphology is obtained for the electrospun $PHBHV_{83}(carv/CD\text{-}IC)_{17}$ (276 $g.L^{-1}$) at 1 $mL.h^{-1}$. Homogeneous fibers without defects were obtained with a diameter of 854 ± 346 nm. As mentioned above, whatever the concentration of complexes, the decrease in the flow rate (from 1.5 to 1 $mL.h^{-1}$) favorably influences the morphology of the fibers. XRD studies were performed on $PHBHV_{91}(carv/CD\text{-}IC)_9$ and $PHBHV_{83}(carv/CD\text{-}IC)_{17}$ (Figure 7) to investigate the effect of the presence of inclusion complexes into PHBHV nanofibers. A peak characteristic of carv/CD-IC around 12° increases with the content of carv/CD-IC introduced in the blend. The crystalline PHBHV molecules are packed in an orthorhombic unit cell in a helical form with space group $P2_12_12_1$. The polymer has a compact and a right-handed helix with a 2-fold screw axis [47-49]. The diffraction profile obtained for the different scaffolds are typical of semi-crystalline polymers and the presence of carv/CD-IC does not affect the crystallization of PHBHV.

The electrospinning of the blend containing $PHBHV_{91}$ $[PolyCD/carv]_9$ was not possible due to the formation of a suspension. To overcome this difficulty, multilayered material was electrospun in three steps (Figure 2) by successively PHBHV, PolyCD/carv and then PHBHV. The advantage of this approach is to have a high concentration of cyclodextrin. The fibers are well defined with few defects. The fiber diameters are 465 ± 172 nm for PHBHV and 421 ± 149 nm for PolyCD/carv (Table 2).

Table 2: Rheology and fiber characteristics

Samples	Flow rate ($mL.h^{-1}$)	Concentration ($g.L^{-1}$)	Diameter (nm)	Porosity (%)	Viscosity (cP)
PHBHV	1.5	150	No fibers		135 ± 4
	1.5	230	465 ± 172	45 ± 10	2550 ± 430
$PHBHV_{91}CD_9$	1.5	220	505 ± 251	66 ± 8	290 ± 8
$PHBHV_{91}CD_9$	1.5	253	884 ± 191	47 ± 1	979 ± 228
$PHBHV_{91}(carv/CD\text{-}IC)_9$	1.5	253	549 ± 287	43 ± 3	3837 ± 775
$PHBHV_{91}(carv/CD\text{-}IC)_9$	1.0	253	423 ± 175	52 ± 3	3837 ± 775
$PHBHV_{91}polyCD_9$	1.5	253	974 ± 385	48 ± 4	397 ± 27
$PolyCD_{89}/carv_{11}$	1	897	421 ± 149	66 ± 8	4660 ± 762

III Radical Scavenging Activity and antibacterial activities

The antioxidant capacity was assessed using the DPPH radical scavenging assay. This method consists in performing reduction of the DPPH radical to its non-radical form in the presence of carvacrol, a hydrogen donating compound (Figure 8A). The solution containing

PHBHV electrospun mat has a purple color, which corresponds to a UV-visible absorbance at 517 nm showing that PHBHV does not present antiradical activity. On the contrary the solutions containing electrospun fibers of $PHBHV_{91}$(carv/CD-IC)$_9$ and [PHBHV-(PolyCD/carv)-PHBHV] became yellow and present a significant antiradical activity due to the presence of carvacrol. The $PHBHV_{91}$(carv/CD-IC)$_9$ film is nevertheless less antioxidant (RSA 55.1%) than the multilayered one due (RSA 88.6%) to its low concentration of carvacrol. The 3-layered [PHBHV-(PolyCD/carv)-PHBHV] is sufficient to ensure optimal antiradical activity. The antibacterial activity of the supports was tested by inhibiting the bacterial growth of *E. coli* and *S. aureus*. (Figure 8B) shows the bacterial growths on the different nanofibers after immersion in the bacterial suspension for 24 hours. The [PHBHV-(PolyCD/carv)-PHBHV] presents better inhibition (20.9% for *E.coli* and 32.9% *S.aureus*) compared to $PHBHV_{91}$(carv/CD-IC)$_9$ (7.9% and 13.6%), with respect to the reference. These results are related with the weight percentage of carvacrol in the material because the $PHBHV_{91}$(carv/CD-IC)$_9$ only contains 1 wt.% of carvacrol inside the nanofibers while the content reaches 11 wt.% in the [PHBHV-(PolyCD/carv)-PHBHV] material.

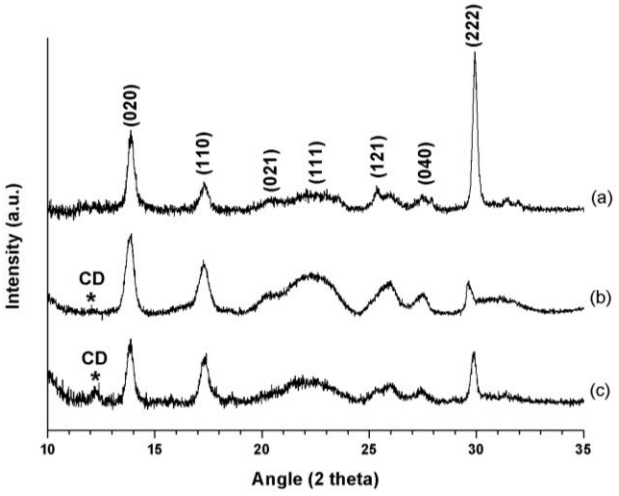

Figure 7: XRD patterns of PHBHV nanofibers (a) $PHBHV_{91}$(carv/CD-IC)$_9$ (b) and $PHBHV_{83}$(carv/CD-IC)$_{17}$ (c)

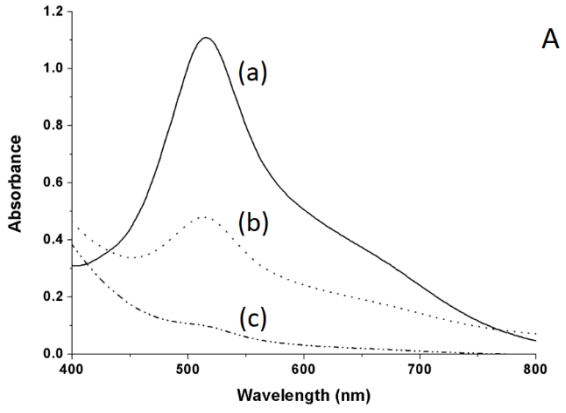

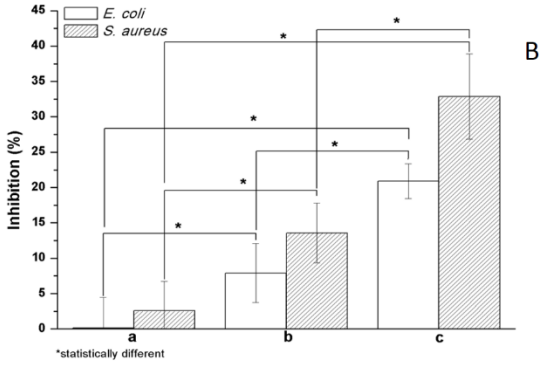

Figure 8: Absorption spectra at 517 nm in presence of DPPH (A), bacterial Inhibition for (a) PHBHV, (b) $PHBHV_{91}$(carv/CD-IC)$_9$, (c) [PHBHV-(PolyCD/carv)-PHBHV] (B)

Conclusion

Electrospun PHBHV nanofibers incorporating carvacrol was successfully prepared by using carvacrol/β-cyclodextrin inclusion complexes. The antibacterial activity and antioxidant properties of the materials are directly relied to the amount of carvacrol included in the hydrophobic cavity of CD. The use of poly(β-CD-epichlorohydrin) polymer, PolyCD, increases the amount of CD and therefore the content of carvacrol. As the electrospinning of the blend containing PHBHV[PolyCD/carv] is not possible due to the formation of a suspension during the process, multilayered material was electrospun in consecutive three steps. The obtained three-layered material [PHBHV-(PolyCD/carv)-PHBHV] is interesting to both ensure optimal antiradical and antibacterial activities and could be advantageously used for enhancing performance of antibacterial materials.

Acknowledgment

We would like to thank Eric Lafontaine for the helpful discussions and the DGA (Direction Generale de l'Armement, France) for the financial support.

References

1. Steinbüchel A, Valentin HE (1995) *FEMS Microbiol Lett* 128: 219.
2. Müller HM, Seebach D (1993) Angewandte Chemie International Edition in English 32: 477.
3. Lee SY (1996) *Biotechnol Bioeng* 49: 1.
4. Chen GQ (2009) *Chem Soc Rev* 38: 2434.
5. Philip S, Keshavarz T, Roy I (2007) *J Chem Technol Biotechnol* 82: 233.
6. Rai R, Keshavarz T, Roether JA, Boccaccini AR, Roy I (2011) *Mater Sci Eng R: Rep* 72: 29.
7. Hazer DB, Kılıçay E, Hazer B (2012) *Mater Sci Eng C* 32: 637.
8. Zinn M, Witholt B, Egli T (2001) *Adv Drug Deliv Rev* 53: 5.
9. Zhang J, Shishatskaya EI, Volova TG, da Silva LF, Chen GQ (2018) *Mater Sci Eng: C* 86: 144.
10. Kurth, N.; Renard, E.; Brachet, F.; Robic, D.; Guerin, P.; Bourbouze, R. Polymer 2002, 43, 1095.

11. Shrivastav A, Kim HY, Kim YR (2019) Advances in the Applications of Polyhydroxyalkanoate Nanoparticles for Novel Drug Delivery System. *BioMed Research International* 2013: 1-12.
12. Nigmatullin R, Thomas P, Lukasiewicz B, Puthussery H, Roy I (2015) *J Chem Technol Biotechnol* 90: 1209.
13. Li Z, Loh XJ (2017) *Wiley Interdiscip Rev Nanomed Nanobiotechnol* 9.
14. Babinot J, Guigner JM, Renard E, Langlois V (2012) *Chem Commun* 48: 5364.
15. Vergnol G, Sow H, Renard E, Haroun F, Langlois V (2012) *Reactive Functional Polymer* 72: 260.
16. Chen GQ, Wu Q (2005) *Biomaterials* 26: 6565.
17. Lemechko P, Ramier J, Versace DL, Guezennec J, Simon-Colin C et al. (2013) *React Funct Polym* 73: 237.
18. Ramier J, Bouderlique T, Stoilova O, Manolova N, Rashkov I, et al. (2014) *Mater Sci Eng C Mater Biol Appl* 38: 161.
19. Ramier J, Boubaker MB, Guerrouache M, Langlois V, Grande D et al. (2014) *J Poly Sci Part A: Poly Chem* 52: 816.
20. Grande D, Ramier J, Versace DL, Renard E, Langlois V (2017) *New Biotechnol* 37: 129.
21. Versace DL, Ramier J, Grande D, Andaloussi SA, Dubot P et al. (2013) *Adv Healthc Mater* 2: 1008.
22. Rodríguez-Tobías H, Morales G, Ledezma A, Romero J, Saldívar R et al. (2016) *J Mater Sci* 51: 8593.
23. Ignatova M, Manolova N, Rashkov I, Markova N (2018) *Int J Pharmaceutic* 545: 342.
24. Kuntzler SG, Almeida ACA, Costa JAV, Morais MG (2018) *Int J Biol Macromol* 113: 1008.
25. Park ES, Moon WS, Song MJ, Kim MN, Chung KH et al. (2001) *Int Biodeteriorat Biodegrad* 47: 209.
26. Nostro A, Papalia T (2012) *Recent Pat Antiinfect Drug Discov* 7: 28.
27. Baser KHC (2008) *Curr Pharm Des* 14: 3106.
28. Beena, Kumar D, Rawat DS (2013) *Bioorganic Medicinal Chem Lett* 23: 641.
29. Iannitelli A, Grande R, Di Stefano A, Di Giulio M, Sozio P et al. (2011) *Int J Mol Sci* 12: 5039.
30. Shakeri F, Shakeri S, Hojjatoleslami M (2014) *J Food Sci* 79: N697.
31. Barba C, Eguinoa A, Ignacio Mate J (2015) *Lwt-Food Sci Technol* 64: 1362.
32. Santos EH, Kamimura JA, Hill LE, Gomes CL (2015) *Lwt-Food Sci Technol* 60: 583.
33. Al-Nasiri G, Cran MJ, Smallridge AJ, Bigger SW (2018) *J Microencapsul* 35: 26.
34. Kfoury M, Landy D, Ruellan S, Auezova L, Greige-Gerges H et al. (2016) *J Org Chem* 12: 29.
35. Kfoury M, Auezova L, Greige-Gerges H, Fourmentin S (2019) *Environ Chem Lett* 17: 129.
36. Mulinacci N, Melani F, Vincieri FF, Mazzi G, Romani A (1996) *Int J Pharmaceutic* 128: 81.
37. Abdelmalek L, Fatiha M, Leila N, Mouna C, Nora M et al. (2016) *J Mole Liquid* 224: 62.
38. Aytac Z, Yildiz ZI, Kayaci-Senirmak F, San Keskin NO, Kusku SI et al. (2016) Food Chem 64: 7325.
39. Renard E, Volet G, Amiel C (2005) *Polym Int* 54: 594.
40. Modjinou T, Versace DL, Abbad-Andallousi S, Bousserrhine N, Dubot P et al. (2016) *React Fun Poly* 101: 47.
41. Rusa CC, Bullions TA, Fox J, Porbeni FE, Wang X et al. (2002) *Langmuir* 18: 10016.
42. Saenger W, Jacob J, Gessler K, Steiner T, Hoffmann D et al. (1998) *Chem Rev* 98: 1787.
43. Kayaci F, Uyar TJ (2011) *Agric Food Chem* 59: 11772.
44. Marcolino VA, Zanin GM, Durrant LR, Benassi MDT, Matioli GJ (2011) *Agric Food Chem* 59: 3348.
45. Tsai Y, Tsai HH, Wu CP, Tsai FJ (2010) *Food Chem* 120: 837.
46. Fong H, Chun I, Reneker DH (1999) *Polymer* 40: 4585.
47. Cobntbekt J, Mabchessault RH (1972) *J Mole Biol* 71: 735.
48. Kaplan DL (1998) Macromolecular Systems - Materials Approach; Springer-Verlag: Berlin Heidelberg, *Biopoly Renewable Res.*
49. Marchessault RH, Coulombe S, Morikawa H, Okamura K, Revol JF (1981) *Can J Chem* 59: 38.